Structural Engineering and Mechanics, Vol. 37, No. 3 (2011) 309-320
DOI: http://dx.doi.org/10.12989/sem.2011.37.3.309

Static behavior of Kiewitt6 suspendome

Kena Li and Dahai Huang*

Department of Civil Engineering, Beijing University of Aeronautics and Astronautics, Beijing 100191, China

(Received March 31, 2010, Accepted October 13, 2010)

Abstract. As a new type of large-span space structure, suspendome is composited of the upper single-layer reticulated shell and the lower cable-strut system. It has better mechanical properties compared to single-layer reticulated shell, and the overall stiffness of suspendome structure increases greatly due to the prestress of cable. Consequently, it can cross a larger span reasonably, economically and grandly with high rigidity, good stability and simple construction. For a better assessment of the advantages of mechanical characteristic of suspendome quantitatively, the static behavior of Kiewitt6 suspendome was studied by using finite element method, and ADINA was the software application to implement the analysis. By studying a certain suspendome, the internal forces, deformation and support constrained forces of the structure were obtained in this paper. Furthermore, the influences of parameters including prestress, stay bar length, cross-sectional area and rise-to-span ratio were also discussed. The results show that the increase of prestress and vertical stay bar length can improve the stiffness of suspendome; Cross-sectional area has nearly no impact on the static behavior, and the rise-to-span ratio is the most sensitive parameter.

Keywords: K6 suspendome; static behavior; influence; prestress; stay bar length; cross-sectional area; rise-to-span ratio.

1. Introduction

In recent years, space structures have been developing rapidly. Reticulated shells and tensegrity structures are widely used all over the world. The suspendome system, which was developed by Kawaguchi, is one of the most attractive space structures due to its excellent structural properties. Suspendome is composited of the upper single-layer reticulated shell and the lower cable-strut system which includes vertical stay bars, radial (oblique) cables and circumferential tensile cables.

The fundamental idea of the suspendome system is the stiffening of a single-layer dome with a tensegrity (cable-strut) system, as is shown in Fig. 1. The upper single-layer shell provides rigid support and decreases the flexibility of the lower cable-strut system, and thus reduces the required prestress force in the cables compared to that of the cable-dome system. Simultaneously, the lower cable-strut system reduces the stress in the members of the upper single-layer reticulated shell. As a result, the capacity of the overall system is enhanced.

The lower cable-strut system stiffens the suspendome system in two different ways. First, the prestressed cables introduce an opposing force to the external gravity load. Another method is to

*Corresponding author, Professor, E-mail: huangdh@mail.tsinghua.edu.cn

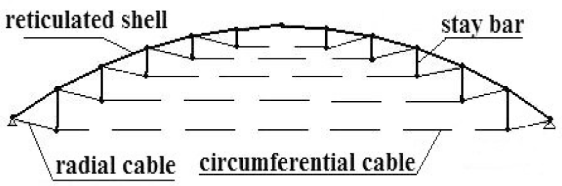

Fig. 1 Diagram of Kiewitt suspendome

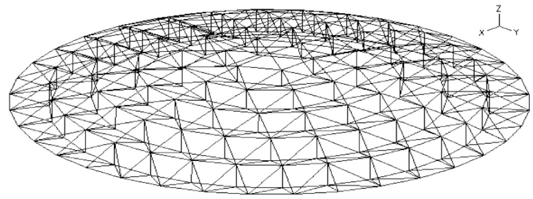

Fig. 2 Kiewitt suspendome

treat the prestressed cables as equivalent pre-tensioned struts. In this way, the suspendome system works like a double-layer dome. Reasonable prestress of circumferential cables lead to upward force of vertical stay bars, and thus the stay bars become vertical elastic support which can greatly reduce the deflection and deformation of the upper shell. Moreover, the circumferential prestressed cables in the outermost ring can generate the inward circumferential tension, therefore the outward pushing force of suspendome applying to the boundary can be significantly reduced (Wang 2003).

The suspendome system has been widely used, with the Hikarigaoka Dome and Fureai Dome in Japan, and the Kiewitt suspendome in Tianjin in China as examples. Moreover, a comprehensive analysis of the modified Kiewitt suspendome has been carried out. Theoretical and experimental research on the mechanical properties of suspendome structure in static and dynamic loads were carried out (Kawaguchi 1999, Tian 2001, Chen 2004) prestress, stay bar length, cross-sectional area and rise-to-span ratio prestress, stay bar length, cross-sectional area and rise-to-span ratio. The initial prestress distribution and stability of suspendome were analyzed in Zhejiang University (Zhang 2004). Furthermore, the capacity of Kiewitt suspendome was investigated in Tsinghua University (Cui 2003), and factors affecting the design and construction of Lamella suspen-dome systems were studied (Kitipornchai and Kang 2005). In addition, Fu (2006) proposed non-linear structural analysis software with functions of the structural analysis and geometrical design of Tensegrity structures, and Satria (2008) discussed the feasibility of a new type of two-way system for single layer lattice domes under earthquake motions which showed the possibility of designing a new type of lattice dome.

Although static and dynamic researches have been carried out, many aspects that are related to the structural characteristics of the suspendome have not been addressed in the literature, such as the effects of parameters on the static behavior, the connection rigidity, and the geometric imperfection on the buckling behavior of the system. The primary aim of this paper is to investigate the static behavior of suspendome system comprehensively, and to provide useful guidelines for engineers in the analysis, design, and construction of this type of structure. A finite element model of a Kiewitt6 suspendome structure is built and its static behavior under concentrated load has been investigated. Then structural parameters of the suspendome, such as prestresses of cables, heights of vertical stay bars, cross-sectional areas of upper bars and rise-to-span ratio of suspendome, which influence the static behavior of suspendome structure, have been studied in this study.

2. Analysis of static behavior

Kiewitt 6 suspendome is suitable for large and medium-span structures because of its symmetrical grid (Shen 1997), hence it is preferred in practical engineering. The static behavior of a suspendome

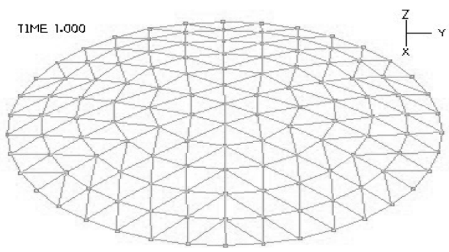

(a) Upper single-layer reticulated shell

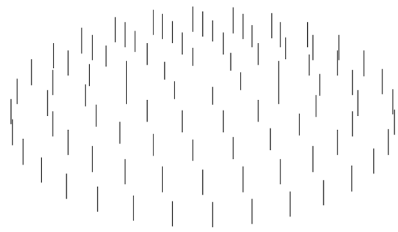

(b) Vertical stay bars

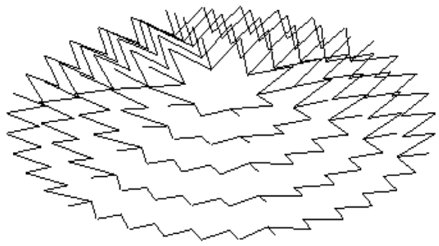

(c) Radial tensile cables

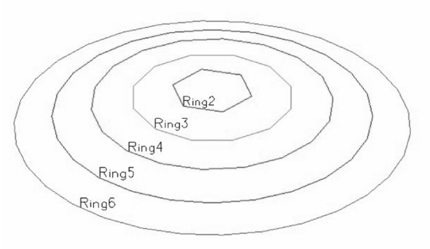

(d) Circumferential tensile cables

Fig. 3 Element groups of Kiewitt 6 suspendome

which is similar to the International business center dome in Tianjin is investigated according to the physical dimension data in literature (Dou 2004), followed by the analysis of the influence of different parameters.

As shown in Fig. 2, the model is a 35.4 m-span and 4.6 m-high K6 suspendome, fixed in the boundary and hinged-jointed at all nodes. Single-layer reticulated shell is composed of Φ133 × 6 circular steel pipes, and vertical stay bars are made up of Φ89 × 4 pipes. There are five rings of circumferential tensile cables, 6 × 19Φ21.5 wire ropes are used in the three internal rings, while 6 × 19Φ24.5 wire ropes in the two external rings. Besides, 6 × 19Φ18.5 wire ropes are used in all the radial tensile cables. Elastic module is defined as 210 GPa for steel pipe and 180 GPa for cable.

The permanent and live load of the roof are about 0.5 kN/m^2 and 1.0 kN/m^2 respectively. According to the static equivalent principle and the uniformity of Kiewitt 6 grid, the uniformly distributed load is equivalent to vertical concentrated load as 10 kN at each node of the upper single-layer reticulated shell.

The initial strain method is applied here because of its briefness and convenience. The tension of the outermost ring is defined as 100 kN in this section, and the optimum ratio of circumferential tensile cables is defined as 0.05:0.1:0.2:0.5:1 from interior to exterior referring to literature (Zhang 2003). According to formula $\sigma = F/A$, where σ represents prestress, F stands for tension, and A is the cross-sectional area of cable, the initial prestresses of circumferential cables can be calculated. The results are 0.121, 0.242, 0.483, 0.931, 1.860 MPa from ring 2 to 6, respectively. Then initial pre-strain can be obtained as 6.7×10^{-7}, 1.34×10^{-6}, 2.68×10^{-6}, 5.173×10^{-6}, 1.03×10^{-5} from ring 2 to 6, respectively.

For the sake of the regularization of analysis, Kiewitt 6 suspendome structure is divided into eight element groups as shown in Fig. 3: Group 1 for the upper single-layer reticulated shell, group 2 for the vertical stay bars, group 3 for the radial (oblique) tensile cables, group 4 for the circumferential tensile cables in ring 2 (the innermost ring of circumferential cables are defined as ring 2, corresponding to the ring 2 of single-layer reticulated shell, while ring 1 is actually the central point), group 5, 6, 7 and 8 for ring 3, 4, 5 and 6 of the circumferential tensile cables, respectively.

2.1 Stress behavior of the suspendome members

According to Table 1 and Fig. 4, rules of internal forces are shown as follows:

a. For member bars of the upper single-layer reticulated shell, internal force achieve its maximum at the main rib between ring 2 and ring 3 (figured as L1 in Fig. 6). It becomes smaller from the inner to the outer rings, and the largest force always arises in the main rib bar in each ring. This is determined by the grid form in which the forces are transferred.

b. For vertical stay bars, radial and circumferential tensile cables, the largest internal forces arise in the outermost ring in main rib, and the closer the bars to the center, the smaller the internal forces. Furthermore, in each ring, internal forces become smaller as the bars or cables are farther away from the main rib.

c. The internal forces of circumferential components in ring 2 and ring 3 are pressure. This is due to the lack of prestress. In order to study the effect of prestress and the role of circumferential tensile cables, truss element which can bear pressure is selected to simulate cable approximatively in this paper.

Table 1 Largest internal forces of every element group

Element group	Value of the maximum internal force (kN)	Position of the component
1	-53.454	main rib bar between ring 2 and 3
2	-6.533	under the outermost ring in main rib
3	28.739	the outermost ring in main rib
4	-2.719	Ring 2
5	-2.771	Ring 3
6	7.870	Close to rib in ring 4
7	47.195	Close to rib in ring 5
8	217.726	Close to rib in ring 6

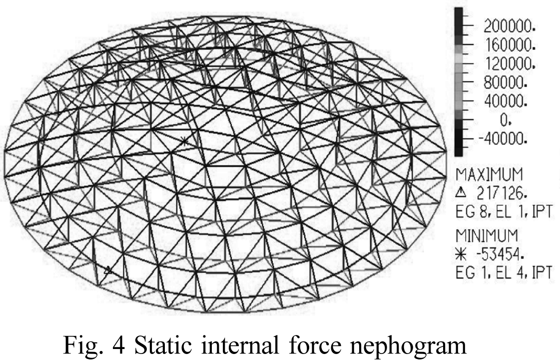

Fig. 4 Static internal force nephogram

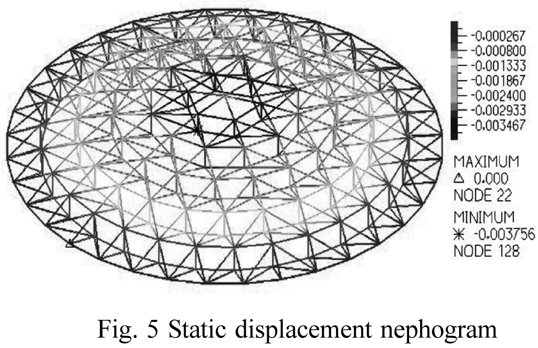

Fig. 5 Static displacement nephogram

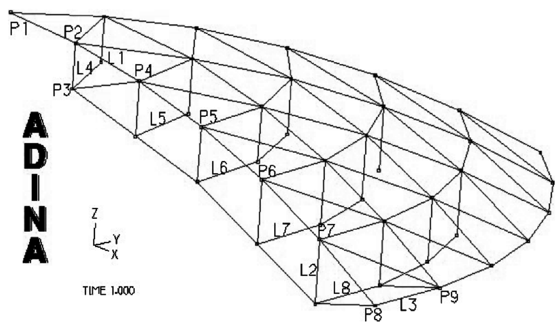

Fig. 6 Typical components and nodes

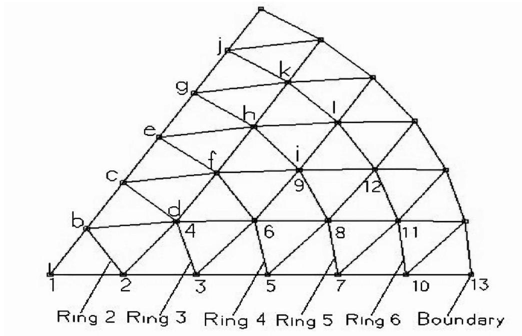

Fig. 7 Nodal position schematic diagram

It can be seen from the next section that the pressures in inner rings are much smaller compared to the outer rings, and have little influence on the internal forces as well as only a little impact on the displacements of some components. The approximation of the cable element would not affect the rules of the structural static behavior. Due to this reason and for the sake of being economical or reducing weight the cables and stay bars in the two innermost rings can be removed sometimes (Zhang 2004).

According to the results and rules of internal forces, the components in which the internal forces are the largest of each group are selected as the representative bars, as shown in Fig. 6.

2.2 Displacement characteristics of nodes

In order to illustrate the rules of nodal displacements clearly, a 1/6 sector of 1/6 of the total is chosen since the suspendome structure is symmetrical. Nodal positions are shown in Fig. 7, where the nodes 1-13 are in the upper reticulated shell, and b-l represent the nodes under the vertical stay

Table 2 Nodal displacements in Z-direction (downwards, mm)

Displacement	Node	Position	Displacement	Node	Position
3.756	2	Ring 2	1.316	9	Ring 5
3.750	b		1.307	8	
3.004	4	Ring 3	1.291	i	
3.000	d		1.283	h	
2.807	3		1.168	7	
2.803	c		1.143	g	
2.676	1	Center	0.689	12	Ring 6
			0.684	11	
			0.625	10	
2.143	6	Ring 4	0.614	i	
2.140	f		0.612	k	
1.973	5		0.545	j	
1.969	e		0.000	13	Boundary

bars in the lower layer. An arrangement of the values of displacements can be found in Table 2.

As recorded in Table 2, it can be seen that the biggest value of nodal displacement is 3.756 mm in the upper reticulated shell of ring 2, followed by the values of nodes in ring 3, and the minimum nodal displacement appear in the outermost ring.

It is clear that the outer the positions of nodes are, the smaller the nodal displacements. Moreover, in the same ring, the farther the nodes are away from the main rib, the larger the displacements, although the values are similar. The exception of the center can be attributed to the composition of the structure, because there is not a vertical stay bar under the central point.

According to the results and rules of nodal displacements, P1 to P7 are selected as the representative nodes as shown in Fig. 6.

2.3 Boundary support constrained forces

Unlike the single-layer reticulated shell, the boundary constrained forces are no longer enormous pushing forces which the structure applies to the external boundary, but turn into pulling forces due to the prestress of cables.

The smallest support constrained forces arise at the main rib nodes, and become larger as the nodes are farther away from the main rib.

3. Analysis of influence of parameters

There is a general consensus that some parameters, such as initial disfigurement, prescribed stress, stay bar length, cross-sectional area and rise-to-span ratio, have more influence on the structure (Kitipornchai and Kang 2005). In this study only four latter parameters are investigated as initial disfigurement has been studied sufficiently by other scholars.

3.1 Influence of prestress on the static behavior

Four prestress conditions are compared in this section, where the prescribed tensions in the outermost circumferential tensile cable are 100 kN, 250 kN, 500 kN and 750 kN, respectively. Then the initial prestress of all circumferential cables can be calculated (Table 3).

From Fig. 8 it can be seen that the largest internal force of the upper reticulated shell decreases slightly with the increase of prestress. Compared to prestress condition 3, the internal forces of bars in the upper shell in condition 4 only decrease by 7.58%, whereas the internal forces of vertical stay bars and radial tensile cables increase obviously by 38.2 and 41.9%. Internal forces of circumferential cables also increase greatly, and the amplitudes of increase become greater and

Table 3 Initial prestresses of circumferential cables (MPa)

	Ring 2	Ring 3	Ring 4	Ring 5	Ring 6
Condition 1	0.121	0.242	0.483	0.931	1.862
Condition 2	0.303	0.605	1.208	2.328	4.655
Condition 3	0.605	1.210	2.415	4.655	9.310
Condition 4	0.908	1.815	3.623	6.983	13.965

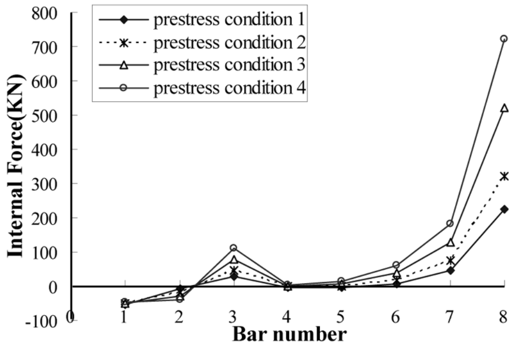

Fig. 8 Internal forces under different prestresses

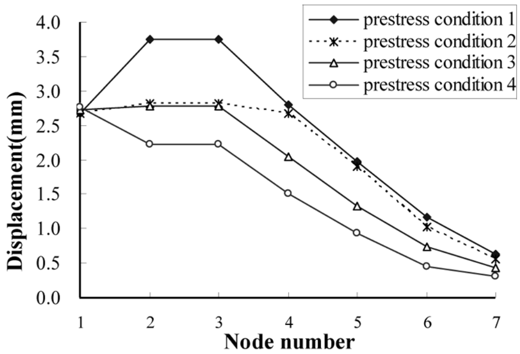

Fig. 9 Nodal displacements under different prestresses

Table 4 Boundary support constrained forces under different prestresses (kN)

Point	Prestress 1	Prestress 2	Prestress 3	Prestress 4
P8	11.659	32.493	73.502	157.296
P9	32.228	50.883	104.182	218.726

greater from outer to inner rings.

Summarized can be said that an increase of the prestress results in little decrease of the internal forces in the upper structure, but a large increase the internal force in the lower structure. This indicates that the increase of prestress can not improve mechanical behavior of suspendome.

In order to explore the optimum range of prestress, the truss element which can bear pressure was selected to simulate cable approximatively. From Fig. 8 and the simulation results, the pressures in inner rings are quite small compared to the outer rings, and moreover they affect little on the internal forces and deformation of other components. This shows that the approximation of the cable element would not affect the rules of the structural static behavior.

In condition 1 the prestress in the outermost ring is 1.86 MPa, and internal forces in the innermost two rings are pressure, which indicate the failure of the cables in ring 2 and ring 3. The appearance of pressure is due to the lack of prestress and the absence of stay bar under the central point. When prestress is raised to 4.7 MPa, the force of the innermost ring has just turned into tension, indicating that all the cables have just become effective. Therefore, the initial prestress of cables in the outermost ring can not be less than 4.7 MPa.

Referring to Fig. 9, displacements of all nodes except the central point decrease obviously as the prestresses of circumferential cables increase. Compared condition 4 to condition 3, prestresses increase by 50%, and thus makes the displacements of P2-P7 decrease by 19.9%, 20%, 26.1%, 30.4%, 38.2%, 28.7%, respectively. The results conclusively demonstrated that the increase of prestress can increase the stiffness, consequently reduce the deformation of suspendome.

It is clear from Table 4 that the boundary constrained forces increase as the prestresses increase. Therefore, the prestress should be controlled to a proper range.

3.2 Influence of stay bar length on the static behavior

As can be seen from Fig. 10, by comparison with the first condition, the internal forces in upper

Table 5 Stay bar lengths of ring 2 to ring 6 (m)

Condition	Ring 2	Ring 3	Ring 4	Ring 5	Ring 6
1	1.2	1.5	1.5	1.8	1.8
2	1.5	1.8	1.8	2.1	2.1
3	1.8	2.1	2.1	2.4	2.4

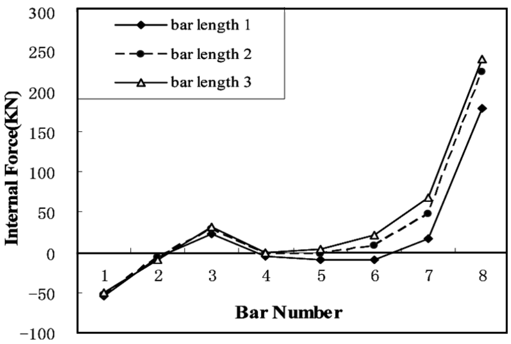

Fig. 10 Comparison of internal forces

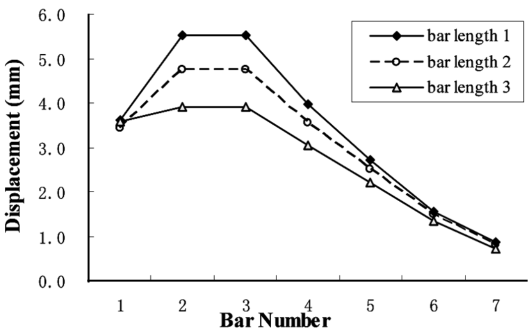

Fig. 11 Comparison of nodal displacements

Table 6 Boundary constrained forces under different stay bar lengths (kN)

Point	Length 1	Length 2	Length 3
P8	10.756	11.659	16.981
P9	27.451	32.228	42.136

layer structure decrease prestress, stay bar length, cross-sectional area and rise-to-span ratio by 3.6%, whereas increase by 8.4% and 23.8% in vertical stay bars and radial cables respectively in the second condition. There is also an obvious increment of internal force in circumferential cables.

This is to say, increasing the length of vertical bar will enlarge the internal forces of most components properly, turn the internal forces of all circumferential cables into tension, and consequently make the structure stress more reasonable. But the vertical stay bar should not be too long, because the slenderness ratios of vertical bars must be restricted to avoid the instability of structure.

Fig. 11 shows that nodal displacements decrease as vertical bar lengths increase. But the biggest change of the displacement between condition 1 and condition 2 is only 14.4%, illustrating that the amplitude of the decrease is small.

It is evident from Table 6 that an increase of the vertical bar length enlarges the constraint reaction of boundary point. The increment of boundary constrained forces is due to the reduction of the angles between radial tensile cables and vertical stay bars.

3.3 Influence of cross-sectional area on the static behavior

Only changing the cross-sectional area of upper single-layer shell pipes and vertical stay bars,

Table 7 Four component cross-sectional area conditions

Condition	Cross section of upper shell	Cross section of stay ball
1	Φ121×5.5	Φ81×3.5
2	Φ133×6	Φ89×4
3	Φ140×6.5	Φ95×4.5
4	Φ146×7	Φ102×4.5

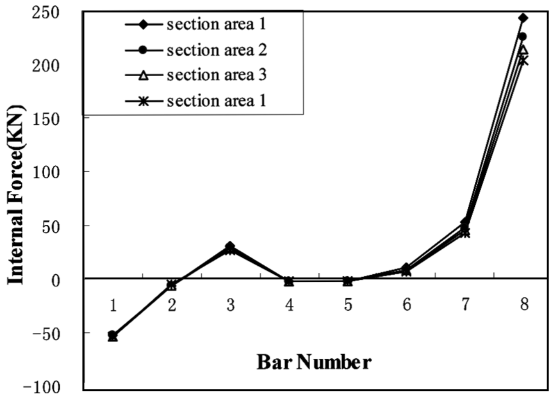

Fig. 12 Internal forces under different cross section

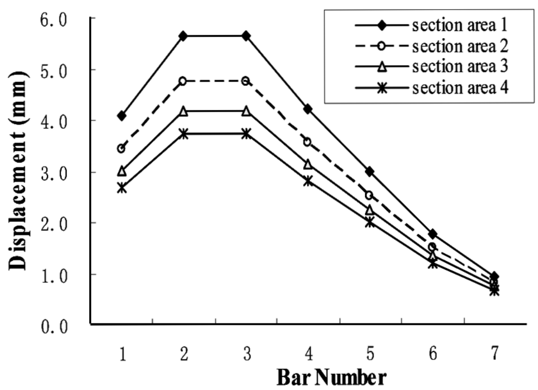

Fig. 13 Nodal displacements under different section

Table 8 Boundary support constrained forces under different sectional area (kN)

Point	Section 1	Section 2	Section 3	Section 4
P8	12.539	11.659	11.182	10.851
P9	35.703	32.228	30.298	28.914

comparison of static behavior in four conditions is performed to investigate the influence of cross-sectional area in this section.

Fig. 12 shows that with the increase of cross-sectional area, the internal forces of upper layer bars, vertical stay bars and circumferential cables increase slightly, while the internal forces of radial tensile cables decrease slightly. The largest change between the first and second condition is only 21.4%, which indicates that the variation of cross-sectional area has little impact on internal forces of structure.

As can be seen from Fig. 13, displacements of typical nodes decrease as the cross-sectional area of pipes increase, Compared the first condition to the second, the range of the change of displacement is from 12.9% to 16.4%. This shows that the increase of cross-sectional area can improve the stiffness of the structure, but not significantly.

From Table 8, it can be seen visually that with the increase of the cross-sectional area of shell pipes and vertical stay bars, the boundary constrained forces decrease. The constraint forces at point 9 decrease by 9.7%, 15.1% and 19.0% respectively in the three latter conditions. This shows that the increase of cross-sectional area improves the performance of suspendome as well as reduces the dependence of the suspendome on the outside boundary.

3.4 Influence of rise-to-span ratio on the static behavior

Suspendome strengthen the single-layer reticulated shell through the introduction of flexible tensile cables. In order to exert the advantages of the cables, the analysis of static behavior under different rise-to-span ratio conditions is accomplished.

Based on the results contained from the computation, comparison of internal forces is plotted in Fig. 14. It can be seen that with the decrease of rise-to-span ratio, the internal forces of most components increase in different degree, among which the increment of circumferential cables in the outermost ring is the biggest. This is because the integral stiffness of suspendome structure decreases as the rise-to-span ratio decreases.

The results in Fig. 15 show that the vertical displacements of all nodes increase largely with the decrease of the rise-to-span ratio. Comparing the first condition with the second, the smallest change of nodal displacements is 30.9% and the largest one is 50.6%. This shows that the ratio of rise-to-span is an important factor on the integral stiffness of the suspendome structure.

It can be seen from Table 10 that the constraint reactions of boundary nodes increase with decreasing the ratio of rise-to-span. The reactions at point 9 in the latter two conditions increase by

Table 9 Heights and rise-to-span ratios of suspendome structure

Condition	Height	Rise-to-span ratio
1	5.9	1/6
2	4.6	1/7.7
3	4.0	1/8.85

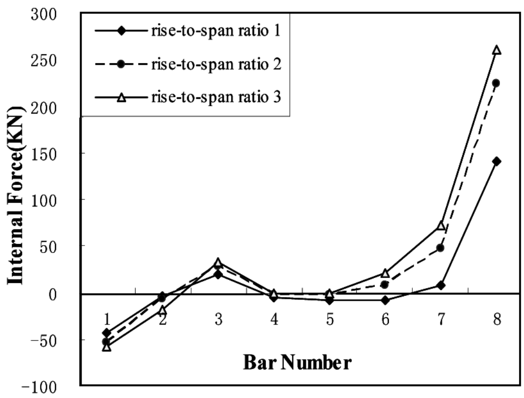

Fig. 14 Internal forces under different ratios

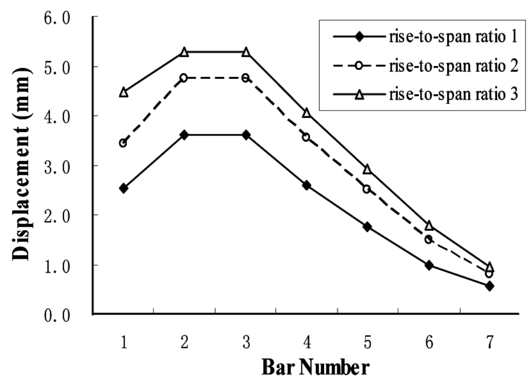

Fig. 15 Nodal displacement under different ratios

Table 10 Boundary support constrained forces under different rise-to-span ratios (kN)

Point	Ratio 1	Ratio 2	Ratio 3
P8	11.326	11.659	15.669
P9	26.791	32.228	41.409

20.3% and 54.6% respectively compared with the first condition. This illustrates the reduction of rise-to-span ratio increases the dependence of the suspendome on the outside boundary.

4. Conclusions

In this study, finite element models of Kiewett6 suspendomes are presented and calculated to investigate the static behavior of suspendome structure. Furthermore, the influence of different parameters such as prestress, stay bar length, cross-sectional area and rise-to-span ratio are discussed. Based on the analysis of static behavior and four parameters of suspendome structure, the following conclusions can be obtained:

1. Under the static load, the internal forces of the bars in upper reticulated shell become smaller, while that of the circumferential tensile cables become larger gradually from inside to outside, as well as from the main rib to the two sides; the rule of the nodal displacement tends to be smaller gradually from inside to outside, and the smallest boundary constraint forces arise at the main rib nodes.
2. Prestress of cables has a big impact on the static behavior of suspendome structure. The increase of prestress can reduce the dependence of the suspendome on the outside boundary effectively, and improve the stiffness obviously, but can not improve the bearing capacity of suspendome. Moreover, its increase would add the burthen of the single-layer shell member bars.
3. The length of the vertical stay bar has a great effect on the static behavior of the suspendome structure. The longer vertical bars are, the bigger the internal forces of the single-layer shell bars, and the smaller the nodal displacements are, hence the larger the integral stiffness of the structure is.
4. The cross-sectional area of shell pipes and vertical stay bars has little impact on the static behavior of the suspendome. The decrease of area can only reduce the nodal displacements and support constraint force slightly.
5. Rise-to-span ratio is the most important parameter of the four parameters. Nodal displacements, internal forces of member bars and the constraint reaction of boundary support increase markedly as the ratio of rise-to-span decreases. The ratio of rise-to-span impacts most on the outermost ring circumferential tensile cables.

References

Chen, Z.H. (2004), "Analysis on structural system and structural properties of the suspendome system", *J. Build. Struct.*, **34**(5), 38-41.

Cui, X.Q. and Guo, Y.L. (2003), "Elastic ultimate capacity of Kiewitt suspendome", *J. Build. Struct.*, **24**(1), 74-79.

Dou, K.L. (2004), *Stability Analysis of Kiewitt Suspendome and Static Tests Researches of Suspendome*; Master Degree Thesis, Tianjin University, Tianjin, China.

Fu, F. (2005), "Structural behavior and design methods of Tensegrity domes". *J. Constr. Steel Res.*, **61**, 23-35.

Fu, F. (2006), "Non-linear static analysis and design of Tensegrity domes", *Steel Compos. Struct.,* **6**(5), 417-433.

Han, Q. and Liu, X. (2002), "Behavior of a single layer spherical dome with openings and large depth-to-span ratio", *Adv. Struct. Eng.*, **5**(3), 137-142.

Kang, W.J., Chen, Z.H. and Lam, H.F. (2003), "Analysis and design of the general and outmost-ring stiffened suspen-dome structures", *Comput. Struct.*, **25**(13), 1685-169.

Kawaguchi, M. and Abe, M. (1999), "Design tests and realization of 'suspendome' system", *J. IASS*, **40**(131), 179-192.
Kitipornchai, S., Kang, W.J. and Lam, H.F. (2005), "Factors affecting the design and construction of Lamella suspen-dome systems", *J. Constr. Steel Res.,* **61**(6), 764-785.
Saka, M.P. (2007), "Optimum topological design of geometrically nonlinear single layer latticed domes using coupled genetic algorithm", *Comput. Struct.*, **85**(21-22), 1635-1646.
Satria, E. and Kato, S. (2008), "Study on dynamic behavior of a new type of two-way single layer lattice dome with nodal eccentricity", *Steel Compos. Struct.,* **8**(6), 511-530.
Shen, Z.Y. and Chen, Y.Y (1997), *The Grid and Reticulated Shell Structure*, Tongji University Press, Shanghai.
Tatemichi, I., Hatato, T., Anma, Y. and Fujiwara, S. (1997), "Vibration tests on a full-size suspen-dome structure", *Int. J. Space Struct*., **12**(3-4), 217-224.
Tian, G. (2001), "The theoretical analysis and practical application research of suspen-dome", Master Degree Thesis, Department of Civil Engineering, Tianjin University.
Yin, D.N. and Liu, S.W. (1996), *Design of Reticulated Shell Structure*, China Architecture and Building Press, Beijing.
Zhang, C.Y. (2003), "Theoretical analysis of suspendome", Master Thesis, Tianjin University, Tianjin, China.
Zhang, M.S. and Dong, S.L. (2004), "Distribution of initial pre-stress and stability analysis of suspendome", *J. Spatial Struct.*, **10**(2), 8-12.
Zhang, M.S. (2004), "Theoretical research on suspendome", Ph.D. Thesis, Zhejiang University, Zhejiang, China.